THE INJECTION BUMPER SYSTEM FOR LEIR ION TESTS

A. Fowler, K.-D. Metzmacher
CERN, CH-1211 Geneva 23, Switzerland

Abstract

After the completion of the antiproton physics program at end of 1996, the Low Energy Antiproton Ring (LEAR) was modified for a final series of experiments to test the lead ion accumulation scheme that is foreseen for the Large Hadron Collider (LHC). One of the goals of these 1997 experiments was to test a new combined transverse and longitudinal multi-turn injection scheme. This required, in part the design and installation of a new injection bumper system. This paper describes the design and achieved performance of a bumper system for the injection of Pb^{54+} ions into the Low Energy Ion Ring (LEIR).

1. INTRODUCTION

The operational characteristics of the multi-turn injection bumper system (1) require a symmetrical arrangement of four deflectors centred on the electrostatic injection septum SEH11. Magnetic deflectors were preferred to electrostatic deflectors owing to the existence of two magnets having already served as bumpers in LEAR; the necessary deflection of 10mrad per bumper being within their operating capability. The bumper positions are shown in figure 1.

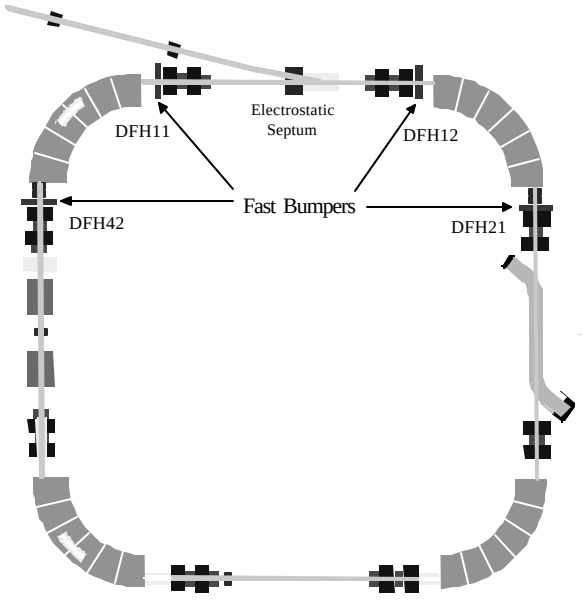

Figure 1. Position of the four injection bumpers (DFH) in the LEIR machine

Bumpers DFH42 and DFH21 require similar magnetic fields, as do bumpers DFH11 and DFH12. The rise of the magnetic field is not critical, provided it is long compared to a betatron oscillation (~1us) and short compared to the 100ms of the Linac repetition time. The fall of the magnetic field required is linear with a 100 - 0% fall-time variable between 14us and 200us in four distinct steps corresponding to 5, 10, 25 and 75-turns of beam in the LEIR machine. A pulse burst repetition rate of 10Hz during 1.2s every 30s was specified.

2. DESIGN PROPOSAL

An existing bumper system (2) previously installed in the LEAR machine for H^-/H^0 injection had been modified for use in preliminary ion injection tests to LEAR in 1994. Its subsequent operating characteristics were sufficiently close to those required for it to be considered for use in this application. However, its operating principle was based on a resonant semi-sinusoidal current discharge into the bumper magnet with a free-wheel diode/capacitor circuit supplementing the falling current edge to produce a quasi-linear slope. The main disadvantage of this system was, that the resonant period of the primary discharge had to be sufficiently short so as not to unduly perturb the linearity of the falling edge of the current. This imposed an upper limit on the value of the primary capacitance (given that the magnet inductance was fixed) and necessitated voltages of the order of 30kV to achieve the required peak magnet current, with consequent large and costly hardware. The advent of new high-current, high-voltage semiconductor switches (Integrated Gate Bipolar Transistors IGBT's) allows a fully switched capacitor discharge. At switch closure the current rises to the peak magnet current at which point the switch is opened and a tuned free-wheel diode/capacitor circuit conducts the falling linear current phase. As no part of the primary capacitor current is present in the linear current phase, the only restriction on the frequency of the primary discharge is that its rise time is short relative to the Linac cycle time. This allows the use of a much larger capacitance, consequently reducing the initial charge voltage required to establish the peak magnet current.

3. CIRCUIT DESCRIPTION

3.1 Pulsed Power Supply

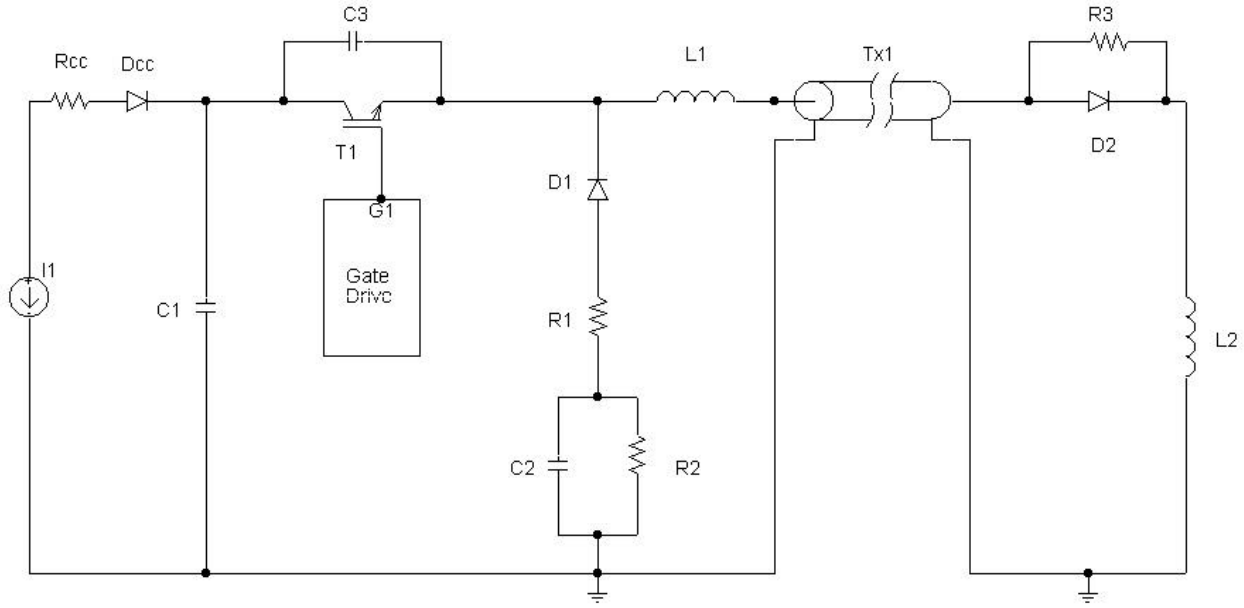

Figure 2. Simplified circuit diagram of one bumper

A simplified electrical circuit for one bumper magnet and its associated power supply is shown in figure 2, above. The operation of the power supply is as follows: C1 is charged to a voltage V via Rcc and Dcc by a current source I1. When the semiconductor switch, T1, is gated on, a resonance is excited between C1 and the magnet inductance L2 in series with L1. This resonant discharge is interrupted by the opening of T1, at which point the free-wheel circuit comprising D1, R1, and C2 begins to conduct. The circuit is still resonant, but the frequency is now determined principally by C2, R1, L1 and L2. An initial current $IL2_{peak}$ is present at the start of this second resonance, and subsequently takes the form $Ie^{-\alpha t}\cos\beta t$;

where $\alpha = \frac{R_1}{2.L_t}$, $\beta = \sqrt{\frac{1}{L_t.C_2} - \frac{R_1^2}{4.L_t^2}}$ and L_t = L1+L2.

Suitable choice of L1 (L2 being fixed), C2 and R1 allows a good approximation to a linear fall of current over the desired time periods. The current is interrupted at the zero crossing due to the opening of diode D1.

Figure 3 below shows a PSpice ™ simulation output for the 5 turns operation. A falling current edge from 1000A to 0A in 14us is required. The top trace shows the current through T1 increasing to the required peak current in the magnet L2, at which point T1 is gated off. At this instant the voltage at the emitter of T1 becomes negative due to the negative di/dt in L2. The second trace shows the freewheel diode circuit beginning to conduct at the instant of T1 opening; D1 changing from being reverse-biased to forward-biased. The third trace shows the current in the magnet, L2, which is simply the sum of the currents in the upper two traces. The lowest trace shows the voltage across T1; of particular note is the large induced voltage seen during the negative ramp of the current.

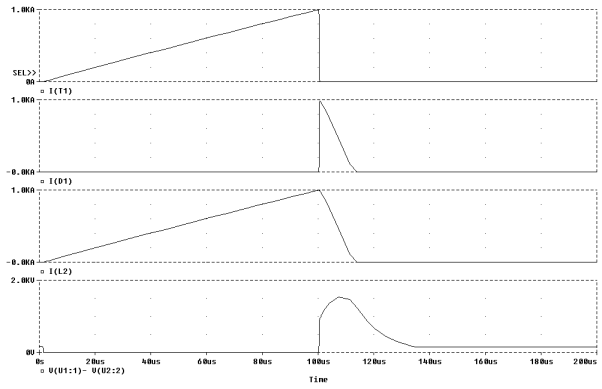

Figure 3. Representative waveforms of the power supply

This induced voltage dictates the use of a high-voltage IGBT, even though the voltage needed on the primary capacitor, C1, is only of the order of 200V. The largest induced voltage across T1 appears in the 5-turns configuration and reaches a maximum of 1600V. A Siemens BSM300GA170DN2 IGBT was chosen with a maximum Vce rating of 1700V, its peak current rating of 880A requiring two such devices connected in parallel.

In order to reduce the inductance of the circuit, and consequently the induced voltages, twenty four coax cables of 20m each were connected in parallel to implement the connection between the power supply and the magnets. This resulted in an additional circuit inductance of 200nH. More cables in parallel would reduce this inductance further but increase the total cable capacitance which has undesirable effects on circuit performance.

The distributed capacitance of the transmission line, Tx_1 is negatively charged at the end of the pulse. A resonance would occur between this capacitance and the magnet inductance, if diode D2 were not present to suppress these post-pulse oscillations in the magnet current. R3 provides a low impedance path to earth for the transmission line capacitance to discharge post-pulse, in order to minimise the duration to which T1 is subjected to large collector-emitter voltages.

Similarly, at the end of the pulse, C2 is negatively charged, having recuperated most of the energy stored in the magnetic field of L2 at the instance of opening T1. R2 allows the dissipation of this energy .

D1 and D2 are both Siemens BYM600A170DN2 diodes with a reverse voltage rating of 1700V and a peak pulsed current rating of 1200A.

C3 is included to suppress potentially destructive voltages induced across T1 during its turn-off.

The configurations of the circuit for the different slope-lengths needed for the LEIR machine operation are achieved by varying the values of C2, R2 and L1. The peak current established in the magnet, L2, is a function of both the primary capacitor voltage, V_{C1} and the duration for which T1 is gated-on (provided this time is less than one-quarter of the primary resonant period). A limit of 300V was imposed by the rating of the 13mF primary capacitor, C1, chosen.

The main parameter values for the four configurations are given in table 1.

	5-turns	**10-turns**	**25-turns**	**75-turns**
Fall-time	14μs	28μs	70μs	210μs
Vc1	160V	160V	215V	240V
T1 gate-time	100μs	100μs	400μs	600μs
L1	0μH	0μH	35μH	70μH
C2	5μF	25μF	55μF	295μF
R1	0.75Ω	0.25Ω	0.35Ω	0.15Ω

Table 1. Values of parameters for the four configurations

3.2 Magnet design

The magnets were originally designed for duty as the PS 50MeV mono-turn injection Kicker Magnet KM30. Two magnets could be recuperated, while two further magnets were newly constructed.

The three piece ferrite C-core and the four turns conductor are moulded together and are enclosed in an aluminium box. Two such C-magnets are mounted face to face to form a window frame magnet. This type of construction permits to easily mount and dismount the assembly around the vacuum chamber. This is of particular interest, as the vacuum chamber has to be regularly equipped with heating jackets and "baked" to obtain the ultra high vacuum (UHV) required to minimise the interaction of the beam with residual gas molecules.

A cross-sectional schematic drawing of the magnet assembly is given in figure 4. From this the wiring arrangement can be seen. In our case the two back-leg windings are connected electrically in series. This results in a rather high magnet inductance, but reduces the magnet current requirement by 50%. Because of the back-leg winding construction the stray inductance is relatively high, amounting to ~53% of the "useful" inductance. The magnet is connected to ground at its low voltage end and its current is monitored with a Pearson ™ current transformer.

The magnetic circuit is split on the vertical centre line, so that the longitudinal coupling impedance is minimised. The split is aluminium filled, thus presenting an efficient eddy current shield for the field induced by the beam.

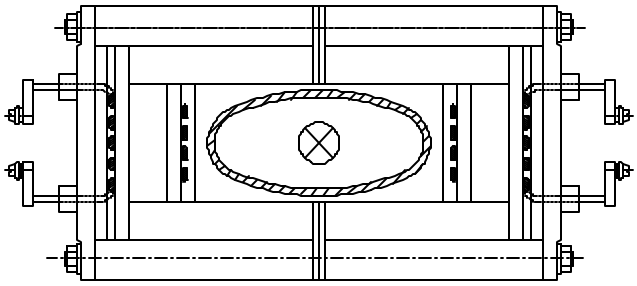

Figure 4. Schematic cross-section of 4-turns magnet

Since the magnet is designed to be installed outside the machine vacuum, the use of a ceramic vacuum chamber is required, because a metal chamber would seriously attenuate and disperse the magnetic fields. However, the chamber must be electrically conductive, thus requiring the ceramic to be internally metallised.

The horizontal field-distribution on the median plane has been calculated for nominal excitation and measured at very low excitation with a strip-line probe; both curves are presented in figure 5, from which the useful horizontal aperture can be evaluated. The design data for the magnet are given in table 2.

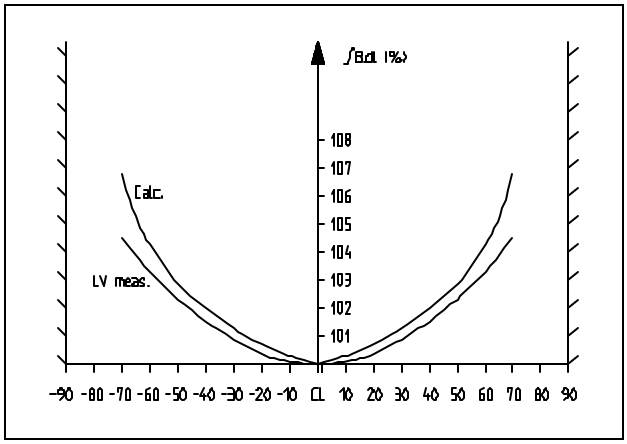

Figure 5. Horizontal field distribution across aperture

Number of magnets/section		One	
Type		Lumped inductance	
Construction		Double C-core with one 4-turn back-leg winding each. Windings connected in series	
Ferrite types		Philips 4A4 / CMD5005	
Magnet box size	w	351	mm
	h	197	mm
	l	225	mm
Physical aperture	w	180	mm
	h	85	mm
	l	225	mm
Inductance	total	13.77	µH
	strays	4.77	µH
	effect.	9	µH
Ferrite length		150	mm
Effective magnetic length		190	mm
Useful horizontal field region	±1%	±40	mm
	±0.5%	±24	mm
Nominal kicker strength		100	Gm
Maximum excitation		1000 x 4	A.turns
Corresponding air gap flux density		582.8	G
Mean ferrite flux density		2374	G
Mean remanent ∫B.dl		> 0.5	Gm

Table 2. Magnet design parameters and the predicted performance

4. PERFORMANCE

Representative current and voltage waveforms taken from (DFH21) for the four required operational configurations are shown below in the oscillograms in figures 6 to 9.

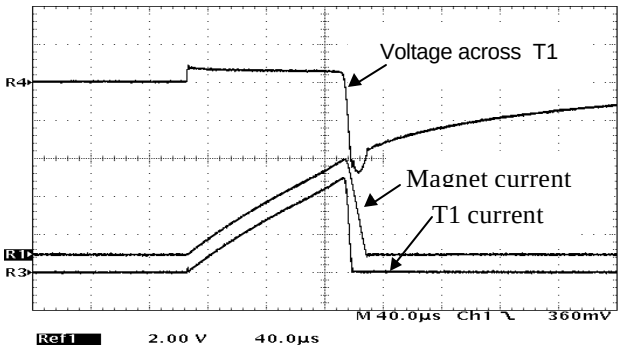

Figure 6. 5-turns configuration, 40us/div.

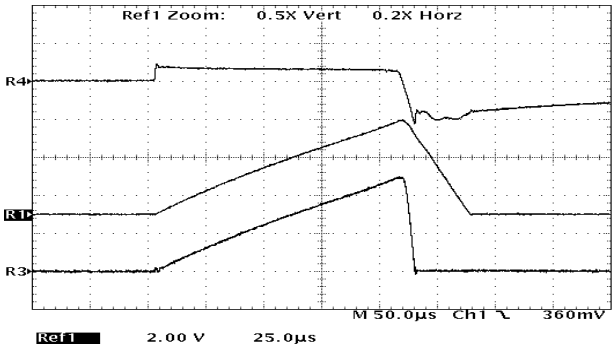

Figure 7. 10-turns configuration, 25us/div.

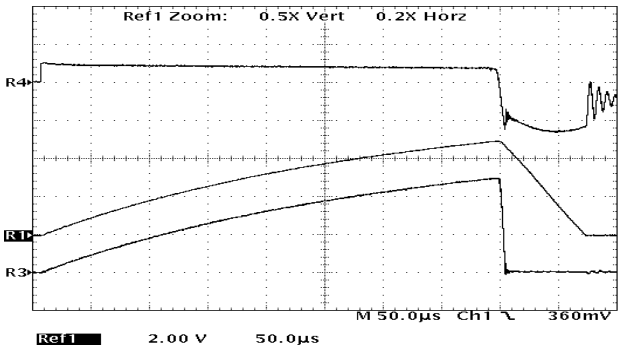

Figure 8. 25-turns configuration, 50us/div.

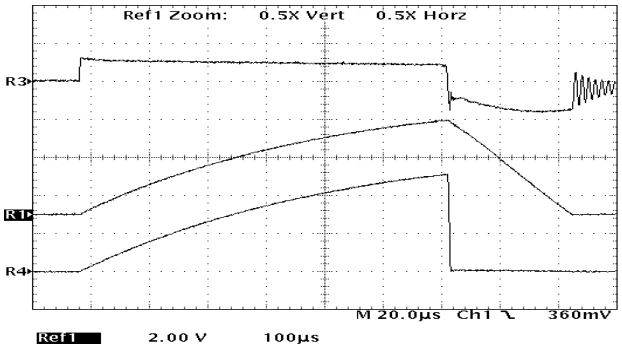

Figure 9. 75-turns configuration, 100us/div.

Figures 10, 11, 12 and 13 show the falling edge currents of all four bumpers, overlaid together with a line representing the ideal linear current.

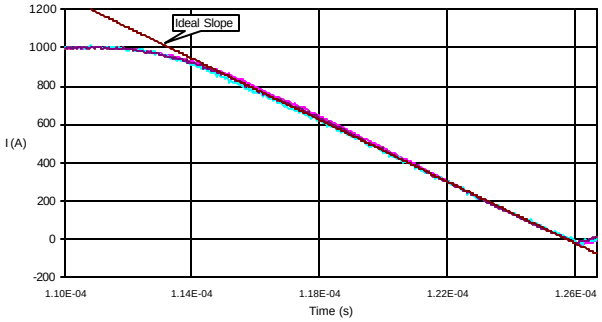

Figure 10. Falling-edge magnet currents in DFH11, 12, 21 and 42, for 5-turns configuration, 4us/div.

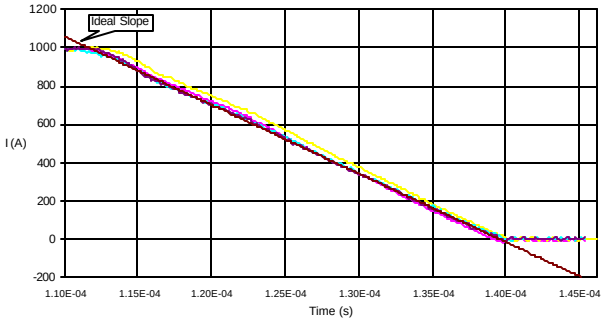

Figure 11. Falling-edge magnet currents in DFH11, 12, 21 and 42, for 10-turns configuration, 5us/div.

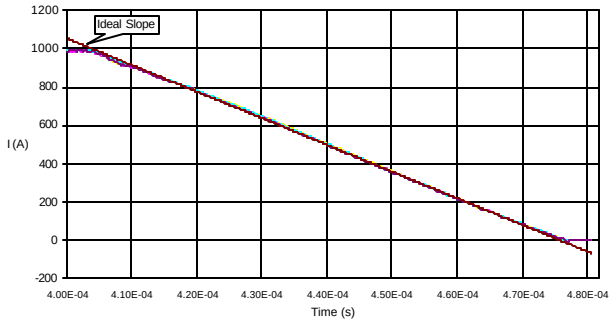

Figure 12. Falling-edge magnet currents in DFH11, 12, 21 and 42, for 25-turns configuration, 10us/div.

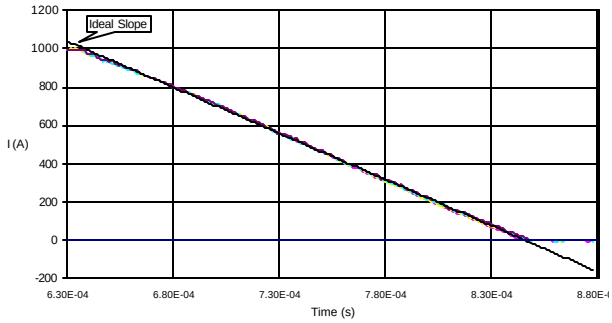

Figure 13. Falling-edge magnet currents in DFH11, 12, 21 and 42, for 75-turns configuration, 50us/div.

The deviation from an ideal linear descent in 14, 28, 70 and 210us (respectively for the 5, 10, 25 and 75-turns schemes) have been calculated from the oscilloscope data. Table 3 below shows the r.m.s deviations for those four configurations.

The r.m.s. falling edge linearity is typically 3% or less; the greater values seen for the 10 turns case are mainly due to poorer alignment of the falling edges (timing discrepancies).

Also shown in table 3 are the tracking deviations of the currents in the two pairs of bumpers, DFH11 v. DFH12, DFH21 v. DFH42. The r.m.s. tracking of the current in these two bumper pairs is below 3% for all four configurations. Figures 14 to 17 show the instantaneous tracking of the bumper pairs.

		Falling edge		Whole pulse
		Rms 90-10%	Rms 95-5%	Tracking r.m.s. (1.)
5 turns	DFH11	2.28%	2.43%	2.27%
	DFH12	2.22%	2.82%	
	DFH21	2.23%	3.04%	2.95%
	DFH42	2.22%	2.82%	
10 turns	DFH11	4.89%	7.43%	1.02%
	DFH12	5.11%	7.58%	
	DFH21	1.82%	2.76%	2.25%
	DFH42	1.99%	2.60%	
25 turns	DFH11	1.03%	1.59%	1.73%
	DFH12	1.12%	1.92%	
	DFH21	0.97%	2.19%	2.00%
	DFH42	1.07%	1.52%	
75 turns	DFH11	3.11%	3.78%	1.81%
	DFH12	2.50%	2.70%	
	DFH21	1.44%	1.82%	2.61%
	DFH42	1.65%	3.23%	

Table 3. R.m.s. tracking deviations evaluated from figures 11 to 17

(1.) The figure is valid for pulse amplitude greater than 10% of Imax. Below this level errors due to noise and oscilloscope resolution have significant influence.

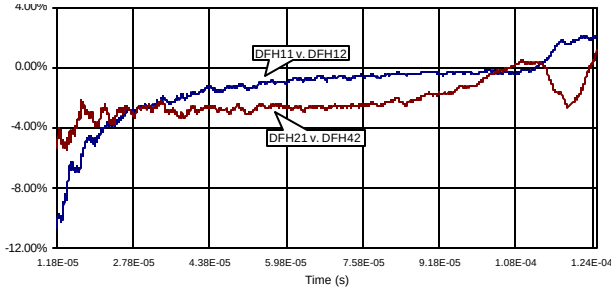

Figure 14. Instantaneous current tracking deviation of the two bumper pairs, 5-turns configuration, 26us/div.

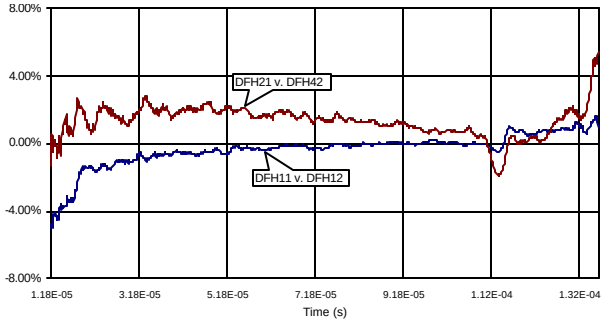

Figure 15. Instantaneous current tracking deviation of the two bumper pairs, 10-turns configuration, 20us/div.

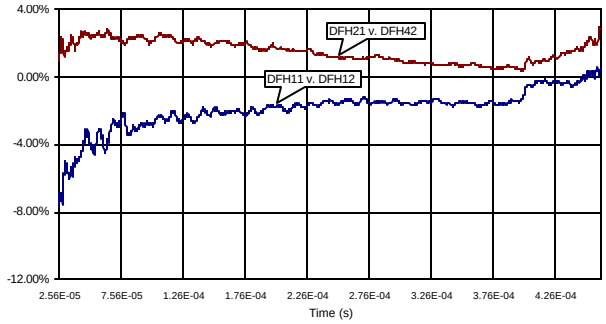

Figure 16. Instantaneous current tracking deviation of the two bumper pairs, 25-turns configuration, 50us/div.

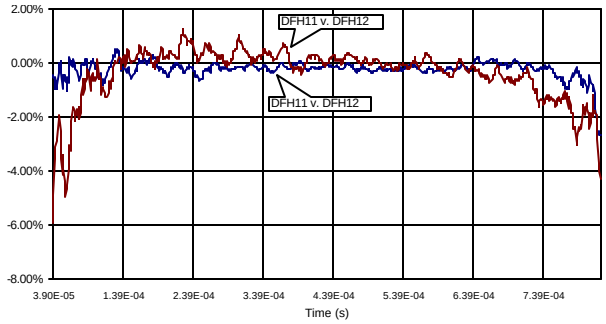

Figure 17. Instantaneous current tracking deviation of the two bumper pairs, 75-turns configuration, 100us/div.

5. SUMMARY

The LEIR multi-turn four-magnet injection bumper system operated successfully during the 1997 LEIR tests with all four different injection turn schemes. This equipment could thus be seen as a prototype injection bumper for an eventual operational system to be used in the context of LEIR providing ion beams for the LHC.
The use of an IGBT-based circuit, instead of the original high-voltage thyratron circuit, resulted in significant reduction of both cost and complexity of the system.

6. REFERENCES

[1] M. Chanel, S. Maury, D. Möhl, *Specification of a LEAR Bump for Multiturn Injection*, CERN/PS 96-04 (Spec.)

[2] D. Grier, K.D. Metzmacher *Design Proposal for a LEAR Bump*, PS/BT/Note 84-3

Distribution list:

PS/CA Technical and scientific staff
J. Bosser
R. Maccaferri
S. Maury
D. Moehl
G. Molinary
G. Tranquille